

Th 10 04

The Application of Full Waveform Seismic Inversion to a Narrow-azimuth Marine Dataset

T. Nangoo* (Imperial College London), M. Warner (Imperial College London), G.S. O'Brien (Tullow Oil Plc), A. Umpleby (Imperial College London), N. Shah (Imperial College London), M. Igoe (Tullow Oil Plc) & J. Morgan (Imperial College London)

SUMMARY

We apply 3D anisotropic acoustic full-waveform inversion to a North Sea narrow-azimuth, marine-streamer dataset. We use a windowed strategy, with 3 stages, first focusing on mainly refracted arrivals with offsets up to (a) 1 km, (b) 2 km and then (c) 3 km with increasing iterations. We demonstrate that our recovered velocity model is realistic.

Overview

3D full waveform inversion (FWI) has been extremely effective when applied to ocean bottom cable data. Such datasets are optimal for FWI as they generally contain low frequencies, long offsets, and full azimuthal coverage, and are rich in refracted seismic arrivals. The vast majority of marine datasets, however, are acquired using towed streamers, which have narrow azimuthal coverage, shorter offsets and reduced signal at low frequencies. In this paper we discuss a methodology for inverting streamer datasets and demonstrate that our recovered inversion velocities are indeed realistic.

We have applied a 3D anisotropic acoustic tomographic inversion algorithm to streamer data from the Dutch Sector of the Southern North Sea, where water depths are approximately 40 m. In this sector, imaging of the deep Carboniferous targets is hindered by rapid changes in velocity, caused by a suite of near surface channels that are located at depths of less than 500 m. These channels produce a strong structural imprint manifested as pull-up effects on what appear to be otherwise smooth reflectors. These shallow channels generate non-hyperbolic sigmoidal gathers. The complexity of the moveout curve, and the short wavelength of the imprint, presents a serious challenge to current traveltimes tomography implementations. It is difficult to pick velocities accurately within channels using standard or conventional techniques, and thus the industry norm is to insert channels manually into the velocity model, guided by the power of the reflection stack. This process is subjective and user dependent, and may lead to inaccurate depth migrations and increased uncertainty in reserve estimates. FWI offers the possibility of simplifying and improving this process, through iteratively converging to a well-resolved velocity model for depth migration. Here, we show that true velocities and positions of the channels are accurately recovered and lead to improved imaging of the shallow overburden, which improves depth migration of the deeper targets.

Methodology and Data

The 3D data were acquired with marine streamers comprising 10 cables each and a conventional dual flip-flop source survey. This study used a subset of the data comprising a total of 3190 shots and 792,000 receivers. The subset has sources with 125 m in-line and 300 m cross-line spacing, and receivers with 100 m in-line and 75 m cross-line spacing. The maximum offset is around 6 km, and the azimuthal coverage is narrow. The inversion is implemented in 3D using a methodology similar to that described by Warner *et al* (2010; 2013). An acoustic finite-difference algorithm is used with a multi-scale approach in the time domain that honours TTI anisotropy which can here be up to 9% to depths of 1000 m.

The field dataset has strong refracted arrivals at all offsets, Figure 1, and the inversion is principally driven by these transmitted arrivals in the low frequency range 4-7 Hz. The data were normalized on a trace by trace basis, such that the inversion fits relative amplitudes in a given trace but not between traces. The data input into the inversion were pre-processed with a high-cut filter and windowed to remove deeper reflections, post-critical refracted arrivals from the deeper chalk interval, and converted shear waves. Initial inversions inverted only data with offsets up to 1 km (Fig. 1b), which was opened up to include 2 km offsets and then offsets up to 3 km at later iterations (Fig 1c). These offsets and times were selected using a phase residual method that avoids cycle skipping (Shah *et al*, 2012).

The data have strong surface multiples which were retained in the inversion. A free-surface modelling condition and a de-ghosted and de-multiplied source signature were used to accurately model these multiples. We tested a contractor's modelled far field source signature, and a signature derived from stacking the short offset field data. Ghosts, first and second order multiples were deterministically removed from the signatures. Both source signatures predicted the data with similar accuracies, and proved to be equally effective in shallow water depths of less than 50 m.

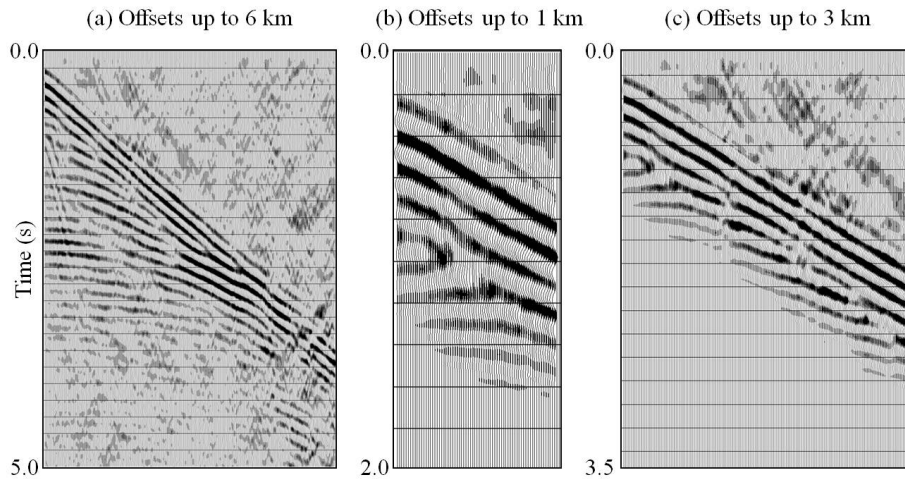


Figure 1 (a) Shot record through the field data with a high-cut filter applied. Transmitted arrivals are the first arrivals at all offsets; these interact with post-critical reflections from the chalk at far offsets. An example of pre-processed field data input into the (b) initial and (c) later inversions; pre-processing included time and offset windowing.

For OBC datasets, the gradient for each shot is calculated, and the gradient for all shots are stacked to form the global gradient. For a streamer dataset, it may be preferential to smooth the gradient in both X and Y. This helps to reduce the strong stripes that are apparent in recovered velocity models; these are acquisition artefacts (Fig. 2). Other techniques that help to reduce these artefacts include using a dataset with a herringbone acquisition geometry as this improves the sampling. The vast majority of field data, however, are acquired with a racetrack geometry due to logistics. Additionally, heavily feathered data may allow for coverage in different directions. Conversely, this may also lead to data gaps in some regions so care would need to be taken in selecting the data for inversion.

Typically source encoding is used to reduce the number of effective shots per iteration and improve the computational efficiency of the inversion. For OBC datasets, use of the principle of reciprocity significantly reduces the number of shots. Additionally, we found that, using fewer shots per iteration and replacing the subset used per iteration either randomly or sequentially such that shots are always distributed throughout the model, is equally as effective and does not have the strong crosstalk associated with source encoding. For this streamer dataset, the sequential reselection of a subset of shots results in a strong, regular interference pattern on the velocity model. This imprint is partially masked by smoothing of the gradient. Randomised rather than regular reselection of the shots is an effective method for dealing efficiently with the large number of shots typical of streamer datasets, and does not produce significant resultant artefacts.

Data coverage is relatively uniform with an OBC dataset. With streamer data, the coverage is not uniform, and on one end of the model the fold is typically greater than the other. This affects the spatial preconditioning and hence the gradient. Weighting the gradient with depth helps to address this lack of coverage.

Results

Figure 2 shows a horizontal slice through the final FWI velocity model, at a depth of 125m below the sea surface. The starting model at this depth was a single constant velocity. Full waveform inversion modifies the background velocity and introduces high-velocity meandering channels. The equivalent depth slice through a PSTM volume obtained using an independent velocity model, shows a similar channel system as does the FWI model with both the gross features and the fine details matched. Notably both methods use different subsets of the data to recover the same channel features. The PSTM uses the sub-critical reflections, and the FWI uses a sparse subset with offsets limited and is

principally driven by the transmitted arrivals. The results were further validated by comparing the trace-to-trace correlation of the synthetic data predicted from the final FWI model and the field data, which show good correlation at all offsets used for the inversion.

Although the FWI recovers geologically realistic channels, there are strong acquisition footprints. Three dominant vertical bands are visible on the FWI model to the left, right and middle of the image in Figure 2, which are due to uneven coverage. Additionally there is a fourth vertical band to the left of the middle band. This imprint is related to the acquisition of the data as it can also be seen in the PSTjioM volume. Horizontal striping is evident throughout the recovered model. This is a residual acquisition footprint due to the separation between shot lines. Smoothing the gradient horizontally by one wavelength is sufficient to remove this imprint. However, this also significantly smoothes away some short-wavelength features that appear to be geologically reasonable. The imprint due to the shot-line separation dominates at all depths, and thus it is preferential to smooth the gradient. However for this study, the recovered velocity model was smoothed before using it in a depth migration algorithm, as this was faster to implement. A V-like stripping pattern corresponding with the sequential shots chosen for inversion is also present in the recovered model. Additionally edge effects are visible at the boundaries of the model, but are not as dominant as the other footprints discussed. The latter are due to the finite aperture of the acquisition system.

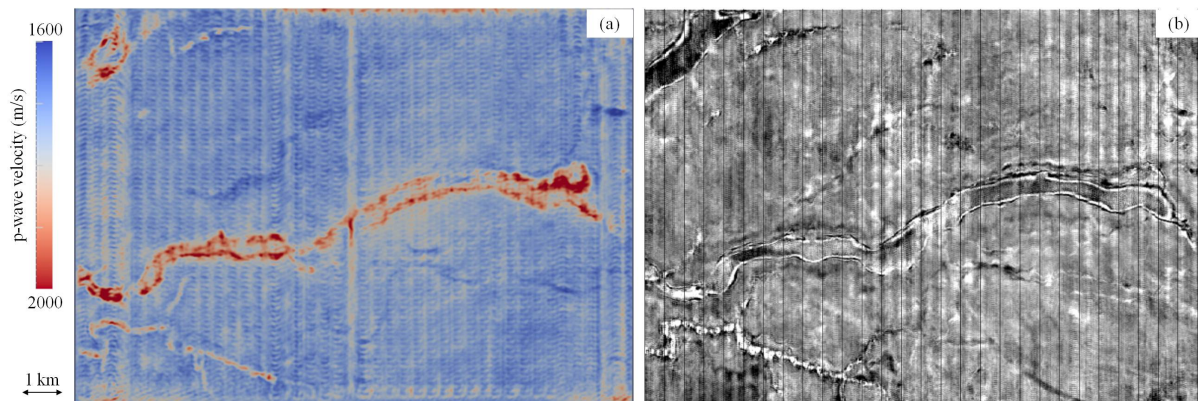


Figure 2 Horizontal slices at 125 m through the (a) FWI velocity model showing the shallow high velocity channels recovered from a single constant velocity, and (b) an independent PSTM volume.

The fundamental question for any FWI study is whether the starting velocity model is adequate, and in particular whether the field data that are available are cycle skipped with respect to the data that are predicted by the starting model, and whether the inversion heads towards the region of the global minimum. We examine this question in Figure 3, using mono-frequency phase residuals, following the scheme of Shah et al (2012). Figure 3a shows phase residuals between the field data and the predicted starting data, displayed at 6 Hz. Figure 3b shows the same information for the final predicted data. In such plots, cycle-skipped boundaries are indicated by sudden jumps from $-\pi$ (blue) to $+\pi$ (red) without passing smoothly through 0 (white).

In Figure 3a, it can be seen that significant portions of the data do appear to be cycle skipped with respect to the starting model. For a typical shot, the data phase residuals are close to zero at the shortest offsets. The residuals then typically become negative with increasing offset, and this trend then reverses, and the phase residual moves through zero to positive values. The data often become cycle skipped at offsets approaching 2000 m, and in some portions of the data, there is also cycle skipping at shorter offsets. If these data are inverted without further precautions, then they will lead to a cycle-skipped final result. As described earlier in the paper, we therefore invert these data in stages, expanding both the offset range and the maximum two-way time as the inversion proceeds, at each stage inverting only those data that appear not to be cycle skipped.

Figure 3b shows the final phase residuals following this process. If FWI has been successful, then the residual should everywhere be small, the area of data initially affected cycle skipping should have shrunk, and cycle-skip boundaries should no longer be apparent within the residual dataset. At offsets of less than 2000 m, it can be seen that these conditions have been met everywhere. At offsets greater than this, there is still however some evidence for the effects of cycle skipping in the centre of the survey. These longest offsets are influenced both by refracted and post-critically reflected arrivals, Figure 1. While the inversion appears to fit the refracted arrivals without cycle skipping, it does not yet fully reproduce the wide-angle reflected arrivals, and it is these that are seen in Figure 3b.

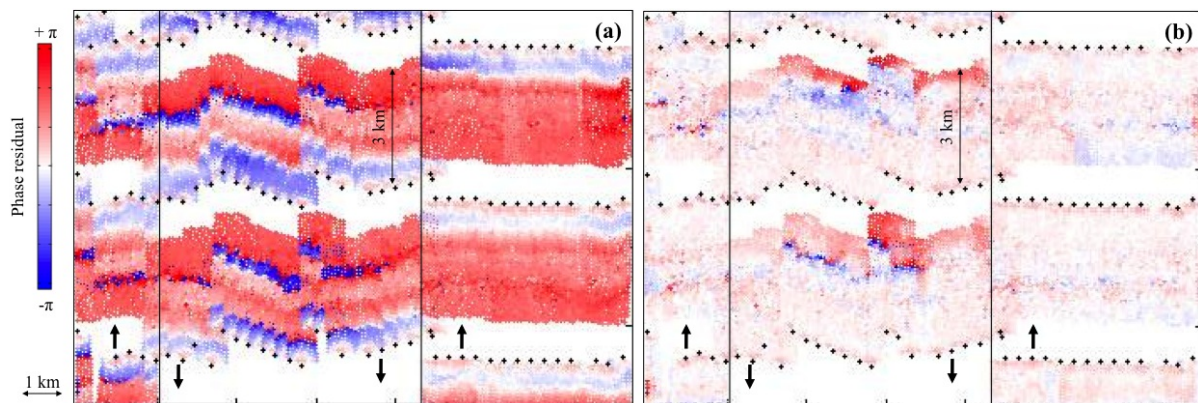


Figure 3 Phase residuals at 6 Hz between the field data and (a) the starting data, and (b) data from the final FWI model. Cycle skipping in these plots is evidenced by abrupt jumps between red and blue. Data from about 100 shots are shown, covering the same area as Figure 2. Shot locations indicated by black dots; sail direction shown by black arrows; first 3 km of offset shown for each shot.

Migration using the shallow final FWI velocity model enhanced the depth migration at both shallow and reservoir depths. In the shallow section, the FWI model generated reflectors without the pull-up effects produced by channels in the shallow overburden, and at deeper reservoir depths, the removal of the distorting effects of the overburden produced a simpler reservoir structure.

Conclusion

Our inversion successfully recovered high velocity channels in the shallow overburden using a widening windowed scheme with offsets up to 3 km in the frequency range 4-7 Hz. The recovered channels are consistent with an independent PSTM, and improve the trace-to-trace correlation between the field and predicted data. Our recovered velocity model improved the depth migration in the shallow, reducing the pull-up effect apparent using conventional methods. The phase residuals suggest that the field data and modelled data are in phase with no cycle skipped boundaries evident.

Acknowledgements

The authors thank Tullow Oil Plc for their kind permission to use their data and publish this work.

References

- Shah, N., Warner, M., Nangoo, T., Umpleby, A., Stekl, I., Morgan, J. and Guasch, L. [2012] Quality assured full-waveform inversion: ensuring starting model adequacy. *SEG Expanded Abstracts*.
- Warner, M., Umpleby, A., Stekl, I. and Morgan, J. [2010] 3D full-wavefield tomography: imaging beneath heterogeneous overburden. *72nd EAGE Conference, Workshop WS6*.
- Warner, M., Ratcliffe, A., Nangoo, T., Morgan, J., Umpleby, A., Shah, N., Vinje, V., Stekl, I., Guasch, L., Win, C., Conroy, G. and Bertrand, A. [2013] Anisotropic 3D full-waveform inversion. *Accepted by Geophysics*.